STABILITY ANALYSIS BY 2D NUMERICAL MODELLING OF A DISSOLUTION CAVERN, RESULTED FROM ROCK SALT EXTRACTION AT OCNELE MARI, ROMANIA

Dacian-Paul MARIAN, Ilie ONICA**, Sorin MIHUȚ****

Abstract: *Ocnele Mari rock salt deposit was mined through dissolving wells in several mining fields, the brine extracted representing the raw material for soda products and chemical products manufactured on the industrial platform Govora. The abandoned fields of dissolving wells represent a real danger, because of the uncontrolled dissolving process that can lead to the development of large caverns, with safety floors which have a thickness that does not correspond in terms of lifting power. This study presents the results obtained from the 2D numerical modelling analysis with finite elements of a large dissolving goal (SOCON Cavern – Ocnele Mari Saline – Romania), cavity resulted from the union of several dissolution goals.*
Key words: *finite element, numeric modelling, stability analysis, rock salt, kinetics dissolution*

1. Overview

From a geographic point of view, the salt that is currently extracted in Romania is almost uniformly distributed throughout the country (Fig. 1).

Fig. 1 *Salt mines map in România* [8]

In Romania, the mining of rock salt deposits has been made during two millennia, through a dry method. Only at the end of the 18th century, at Cacica, they had begun the rock salt mining in solution by evaporation of the brine from the salt springs in the area. After nearly a century rock salt mining started by dissolution in three circular basins with a diameter of 100 m, set-up in underground workings. Ocnele Mari salt deposit was mined by dissolving wells in several drilled wells fields, the brine extracted representing the raw material for soda products and chemical products manufactured on the industrial platform Govora. Extracting the rock salt through wells, as brine, represents a simple method with certain advantages than that of rock salt extraction, in a solid state, through mining workings. The effectiveness of this process consists of low production prices, minimum transportation costs, the opportunity to mine the rock salt deposits with rocks inclusions and deep mining depth. However, insufficient knowledge of the problems regarding the rock salt mining by dissolution can lead to loss of control over the dissolution and the destruction of the pillars among the dissolving chambers [8], [10], [11].

* *Lect.eng.Ph.D, University of Petroșani*
** *Prof.eng.Ph.D, University of Petroșani*
*** *Eng.Ph.D D&M General Construct*

2. Rock salt extraction at Ocnele Mari by dissolution

2.1. Description of the dissolving wells fields from Ocnele Mari

Once Govora plant was set in motion the need for salt in solution increased from 850 000 tons/year to 2 450 000 million tons/year [10].

To meet this need, 4 well fields have been put into operation since 1960, located in the central part of the salt deposit (figure 2).

These well fields are as follow [3], [17], [21], [22]:

a) **Field I -** comprises a total of 10 individual wells, S351 - S360, set-up on Urzicaru Hill. These wells have been exploited during 1960 - 1973 through a mining method with lifts in small scales (stages).

b) **Field II -** comprises a total of 15 individual wells, S361 - S370, S376 - S379 and S381 set-up around Field I, extending eastward in Ţeica district. These wells have been exploited during 1968 - 1991 through a mining method with lifts in big scales (stages).

c) **Field III -** comprises a total of 33 wells, namely:

- a total of 28 individual wells exploited through a mining method with lifts in big scales (stages), divided according to the area where they were set-up and according to the place of connection to the technological installations that serve them as follows:

- *Ţeica Area I* - comprising 5 wells (S401, S402, S404, S405 and S411) set-up on Ţeica Hill, north of the wells that form Fields I and II, connected to the control room of Field II;
- *Ţeica Area II* - with a total of 6 wells (S406 - S410 and S412) set-up on the right side of Ţeica Valley, which were initially connected to a temporary primer station and then to the control room of Field III of wells set-up in Lunca district;
- *Lunca-Goruniş Area* - comprising a total of 17 wells (S403, S413 - S428) set-up in the districts with the same name, connected to the control room of Field III Lunca.

- a total of 5 experimental wells set-up as follows:

- 2 wells (S429 and S430) set-up in Lunca district on the left side of Sărat Brook, located in an isolated area than the individual wells. In regards to these wells, a battery mining method was applied. These two wells were stopped in 2001, having exhausted their reserves.
- 3 wells with channel exploitation (S431, S432 and S433) set-up on Goruniş Hill, south-west of the individual wells, in an isolated area.

d) **Field IV** - which comprises a total of eight wells (S466 - S473) set-up on the perimeter of the former salt mine at Ocniţa, mine partially collapsed, around the lake formed on the old brine pit. The exploitation in this field was done in order to mining the salt reserves abandoned under the old mines and it began in 1992, as it followings: S466-S472 wells; S470-S471 wells; S467-S468-S469 wells, indicating that the S467 well was maintained suspended because the connecting channel between S467 well and S466-S472 wells was executed at another insertion.

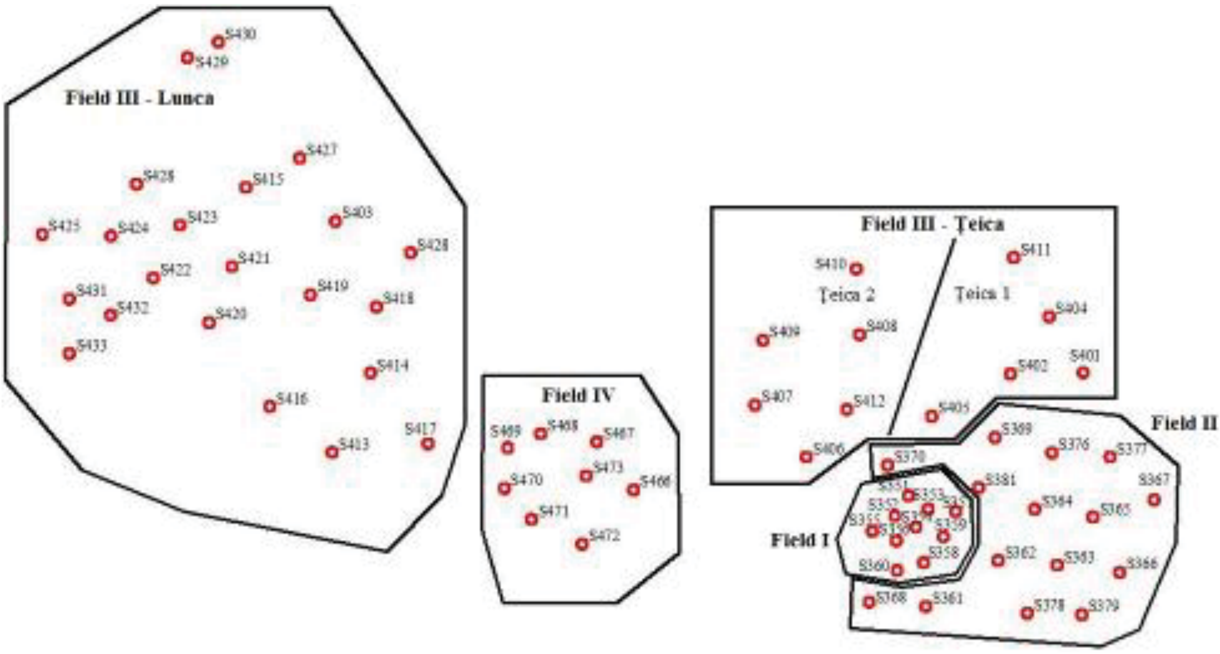

Fig. 2 *Set-up of wells fields from the Ocnele Mari*

2.2. The effects of rock salt extraction by dissolution

Due to dissolving chambers that emerged because of the rock salt mining through the kinetics dissolving wells method, certain peculiar problems appeared regarding the stability of massive rocks. By creating dissolving cavities, the initial state of stress of the massive rocks changes, so that a redistribution of stresses around the created cavity occurs, which leads to the coming out of several stress concentrators. These have the maximum value in the horizontal extremities of the cavity, which could lead to cracking or rock fall from the ceiling or from the dissolving cavity walls [1], [2].

To maintain the balance of massive rocks, both during and after the exploitation, the mining technology must be properly selected according to local geo-mining properties. It is, therefore, necessary to properly establish the dissolving chambers' size and position in the plan. Therefore, if the sizes of the dissolving chambers and the safety pillars among these chambers are designed properly, it can ensure the stability of the excavations over a long period of time [3].

The main negative effects that may result from the exploitation through kinetics dissolution of the rock salt deposits are the following [4], [9], [24]:

- dissolution of the pillars among the dissolving chambers, the joining of the dissolving

chambers could lead to the appearance of several large underground caverns;
- uncontrolled surface subsidence, with the emergence of large caving cones;
- degradation of surfaces and, as well as, of the civil and industrial objectives in that area;
- local saturation of the surface with brine and diesel (or even environmental disasters) due to tightness loss of certain dissolving wells or due to accidental leakage flows.

3. SOCON cavern's stability analysis by 2D numerical modelling

For achieving calculation models with finite elements in plane deformation and in the elastic, isotropic and linear behaviour hypothesis, the CESAR-LCPC 2D software was used [12], [14], [15].

With the help of this software finite element models were accomplished keeping, as much as possible, the geo-mining conditions found in Ocnele Mari rock salt deposit.

3.1. Achievement of numeric models

For a more precise analysis, two numeric models with finite element were made (fig. 4-5) corresponding to sections 3-3` and 6-6` (fig. 3).

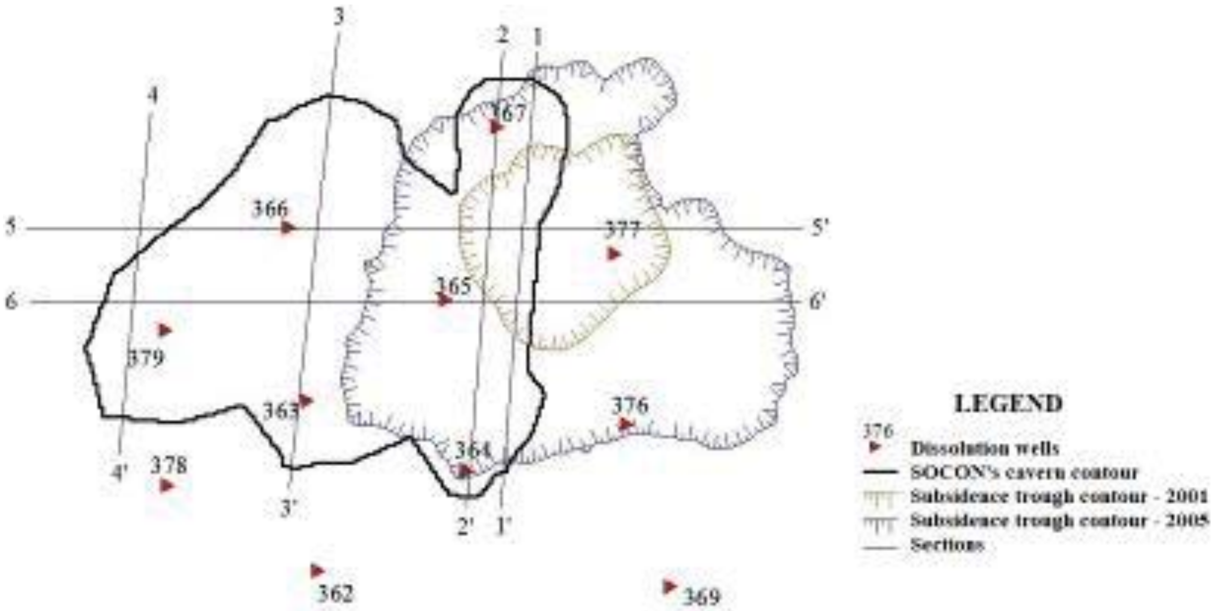

Fig. 3 *Vertical section's position in the plan in regard to SOCON cavern's outline*

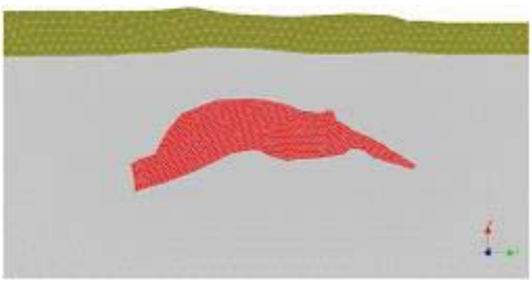

Fig. 4. *Model with finite element SOCON cavern, section 3-3` (Option I)*

Fig. 5. *Model with finite element SOCON cavern, section 6-6` (Option I)*

For SOCON cavern's stability analysis in plane deformation, in the case of the two executed sections, it has been taken into account four options of calculation, namely (Mihuţ, 2015): ***Option I*** – the cavern is completely filled with brine; ***Option II*** – at the top of the cavern (it is considered at a height of 10 m) there is an area with air; ***Option III*** – the cavern is completely filled with brine and the piezometric load in the cavern is located at an elevation of + 290 m; ***Option IV*** – the cavern is completely filled with brine and the piezometric load in the cavern is located at an elevation of + 295 m.

The initial load conditions of the model were considered geostatic $\left[\sigma_o\right]$, corresponding to an average disposition depth of the cavern of approximately H = 125 m, namely:

- vertical geostatic tensions $\sigma_{oy} = \rho_s \cdot g \cdot H = 24806$ kN/m^2 = 24.8MPa;

- horizontal geostatic tensions $\sigma_{ox} = \frac{\nu}{1-\nu} \cdot \sigma_{oy} = k_o \cdot \sigma_{oy} =$ 8269kN/m^2 = 8,3MPa (where $k_o = \frac{\nu}{1-\nu} = 0.333$).

The induced tensions by the presence of excavations resulting from the extraction of salt were $[\sigma_e]$, respectively the tensions variation represented by horizontal tensions σ_{ex} = – 8,3MPa and vertical tensions σ_{ey} = – 24,8MPa. Finally, the loading of models were made with total stresses state (fig. 6): $[\sigma_T] = [\sigma_o] - [\sigma_e]$ [10].

For determining the third dimension, a Lambda coefficient was introduced, determined by relation 1, the value of which was: for section 3-3`: $\lambda = 0.554$ for section 6-6`: $\lambda = 0.618$.

$$\lambda(x) = \frac{1 - th\,(0{,}33 - x/D)}{2} \qquad (1)$$

where: *th* is the hyperbolic tangent; *D* – excavation opening; *x* – the distance from the studied section to the adit end ($\lambda > 0$ if the section is in the rear of the adit end - excavated section; $\lambda < 0$ if the section is in front of the adit end – unexcavated section).

Because inside of the cavern there is a certain amount of brine (which exerts some pressure on the cavern walls), inside the numerical models was inserted a hydrostatic pressure (opposite to that induced by the presence of the excavation) considering zero pressure at the top of the cavern, for option I, respectively 10 m below the top for option II. For options III and IV zero hydrostatic pressure was considered at an elevation + 290m respectively + 295m (fig. 6). The bulk density of the brine taken into account was of $\rho = 1300$ kg/m^3 [7], [18], [19].

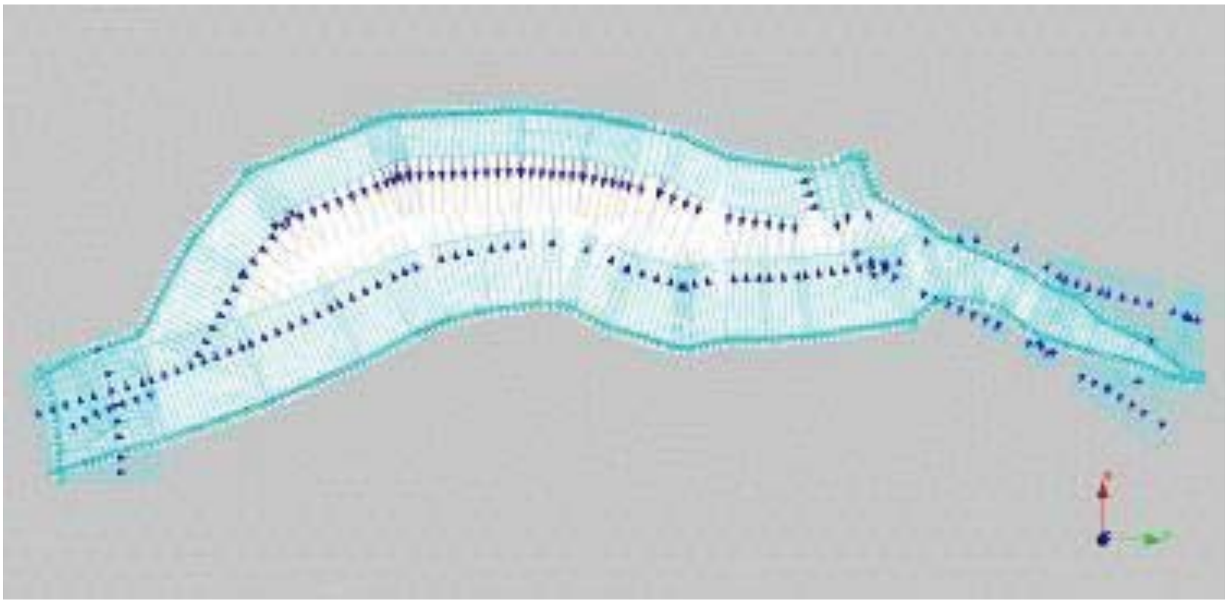

Fig. 6 *The hydrostatic pressure for section 3-3` - Option IV*

To optimize the calculations based on the accuracy of the results required by the stability analysis, calculations were made assuming a total of 60 iterations per increment and a 1% tolerance of the results, using the "initial stress method" for solving the calculations.

3.2 Analysis of the results

After solving the calculations using the models described above, comparing the values of the obtained results (table 1and 2), it may be noted that there aren't major differences between the obtained results in options I and II (Option I – the cavern completely filled with brine; Option II – at the top of the cavern there is an area with air) or between options III and IV. However, major differences are found between options II respectively IV (that is, between option II where the cave is said to have a 10 m cavity at the top and option IV where the hydrostatic pressure in the cavern is at an elevation of + 295 m). Between these two options, there is a difference of about 60%.

As can be seen, the worst case is that where the hydrostatic pressure in the cavern is low, and where at the top of the cavern there is a cavity. Also, you can see that there are great differences between the displacement values and the stress values resulted in the two sections through the cavern, the values of the parameters resulted in section 6-6` being almost four times higher than the values resulted in section 3-3`.

Table 1 *The range of the main calculation parameters from the numerical models, section 3-3'*

Parameter	Range			
	Section 3-3`			
	Option I	***Option II***	***Option III***	***Option IV***
u, [mm]	+324 ÷ -335	+331 ÷ -344	+120 ÷ -124	+108 ÷ -122
v, [mm]	+150 ÷ -1090	+150 ÷ -1110	+48 ÷ -391	+43 ÷ -350
d_{uv}, [mm]	0 ÷ 1090	0 ÷ +1110	0 ÷ +391	0 ÷ +350
σ_{xx}, [kN/m^2]	+4800 ÷ -12700	+4900 ÷ -12900	+4110 ÷ -6910	+4240 ÷ -6560
σ_{yy}, [kN/m^2]	+100 ÷ -34000	+100 ÷ -34900	+100 ÷ -14700	+100 ÷ -13500
σ_{xy}, [kN/m^2]	+8500 ÷ -10200	+8700 ÷ -10400	+3380 ÷ -4070	+3080 ÷ -3710
σ_1, [kN/m^2]	+4990 ÷ -8120	+5090 ÷ -8210	+4310 ÷ -5270	+4420 ÷ -5100
σ_2, [kN/m^2]	+100 ÷ -34600	+100 ÷ -35500	+100 ÷ -15100	+100 ÷ -13900
$\tau_{f\,max}$, [kN/m^2]	0 ÷ +13700	0 ÷ +14100	0 ÷ +5390	0 ÷ +4900
σ_t, [kN/m^2]	0 ÷ +4990	+5080 ÷ -10	0 ÷ +4300	0 ÷ +4420
σ_c, [kN/m^2]	0 ÷ -34600	0 ÷ -35500	0 ÷ -15100	0 ÷ -13900

Tabel 2. *The range of the main calculation parameters from the numerical models, section 6-6'*

Parameter	Range			
	Section 6-6`			
	Option I	***Option II***	***Option III***	***Option IV***
u, [mm]	+1350 ÷ -1150	+1380 ÷ -1190	+904 ÷ -765	+876 ÷ -740
v, [mm]	+420 ÷ -4430	+440 ÷ -4550	+280 ÷ -2980	+280 ÷ -2890
d_{uv}, [mm]	0 ÷ 4440	0 ÷ +4550	0 ÷ +2980	0 ÷ +2890
σ_{xx}, [kN/m^2]	+11100 ÷ -64000	+11500 ÷ -65800	+8100 ÷ -45200	+8000 ÷ -44000
σ_{yy}, [kN/m^2]	+1300 ÷ -90600	+1600 ÷ -93300	+100 ÷ -63400	+100 ÷ -61700
σ_{xy}, [kN/m^2]	+38700 ÷ -33200	+39900 ÷ -34200	+26400 ÷ -22200	+25600 ÷ -21600
σ_1, [kN/m^2]	+11100 ÷ -31300	+11500 ÷ -32100	+8600 ÷ -23000	+8600 ÷ -22500
σ_2, [kN/m^2]	0 ÷ -110000	0 ÷ -113000	+100 ÷ -76500	+100 ÷ -74500
$\tau_{f\,max}$, [kN/m^2]	0 ÷ +40700	0 ÷ +42000	0 ÷ +27800	0 ÷ +27000
σ_t, [kN/m^2]	0 ÷ +11000	0 ÷ +11500	+8620 ÷ -10	+8540 ÷ -10
σ_c, [kN/m^2]	0 ÷ -110000	0 ÷ -113000	+100 ÷ -76500	+100 ÷ -74500

Analysing the massive rocks' vertical displacement values (for the worst case section 6-6` Option II - fig. 7), it appears that the highest embedding is registered in the centre of the cavern, but in reality the caving of the surface area occurred at the edge of the cavern towards the upstream (figure 8).

A possible reason for the caving of the surface in this area could be a horizontal displacement, which, as can be seen in fig. 9 in that certain area it reaches a maximum value (which in the worst case it amounts to 1190 mm). Horizontal displacement leads to the massive rocks' cracking, thus facilitating water infiltration into the cavern and thus dissolving the salt floor.

Studying the massive rocks' tensile stresses in section 6-6` (fig. 10), it can be seen that the surface maximum stresses reach a value of 3500 – 4500kN/m^2, value much above the tensile strength of rocks (approximately 500kN/m^2), these maximum values were registered towards the upstream, approximately around the area that collapsed in 2001.

Predefined sections were executed in accordance with the caverns' ceiling (fig. 11, 12) and the surface area (fig. 13), for a better assessment of the state of stresses, comparing the tensile and shear stress' charts with the limit values of rock salt.

Fig. 7 *Vertical displacement of the massive rocks in section 6-6` scalar representation (Option II) – v, in mm*

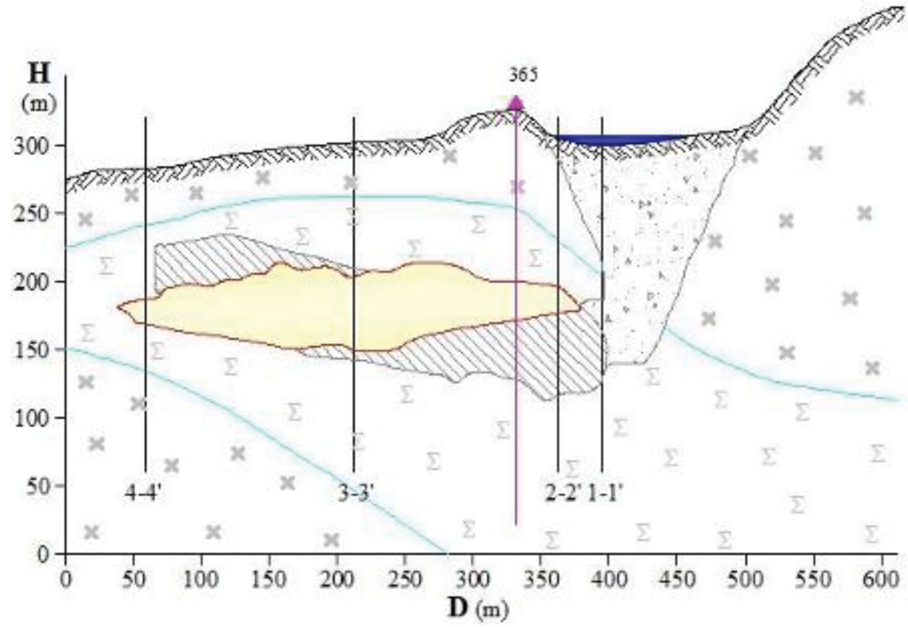

Fig. 8 *Caving of the surface in the wells field II - section 6-6`*

Fig. 9 *Horizontal displacements in section 6-6` scalar representation (Option II) – u, in mm*

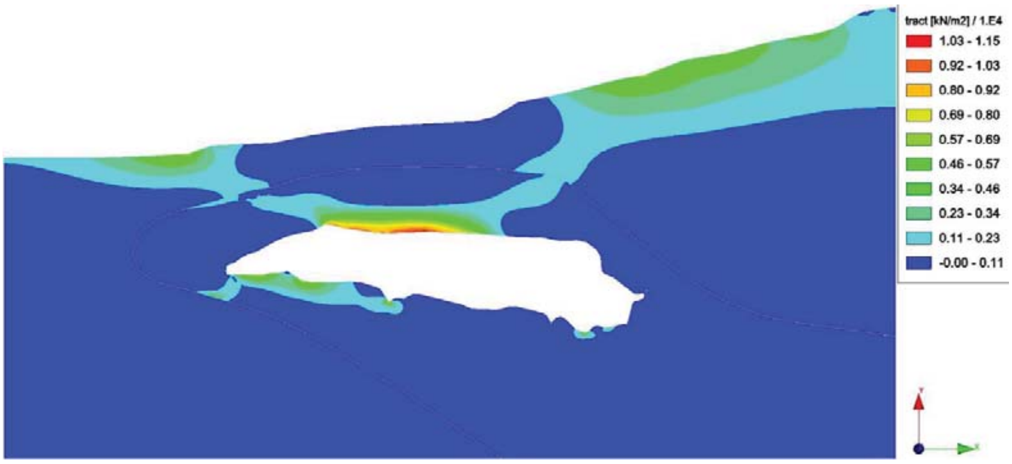

Fig. 10 *Tensile stresses in section 6-6` scalar representation (Option II) -* σ_t *, in kN/m*^{2}

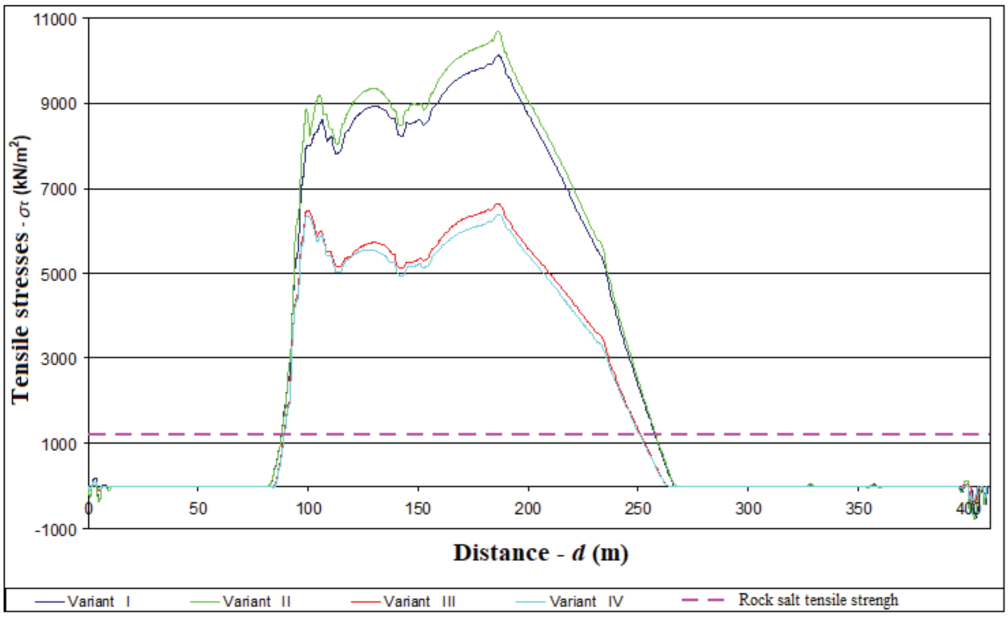

Fig. 11 *Tensile stresses* σ_t *at the cavern's ceiling in section 6-6`*

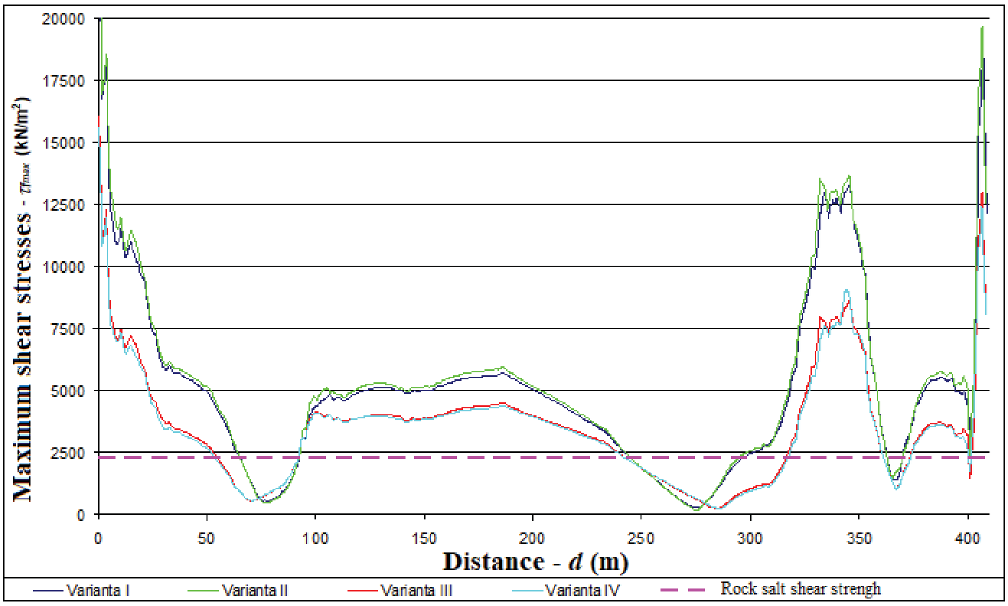

Fig. 12 *Maximum shear stresses* $\tau_{f_{max}}$ *at the cavern's ceiling in section 6-6`*

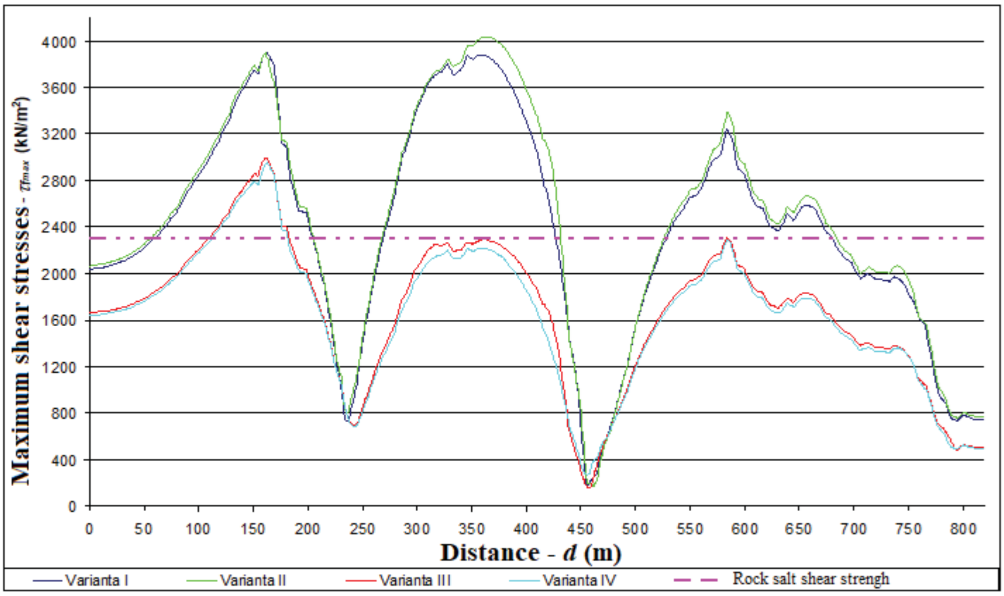

Fig. 13 *Maximum shear stresses* $\tau_{f_{max}}$ *at the surface in section 6-6`*

3.3. Surface stability analysis based on safety coefficients calculated with the Mohr-Coulomb breaking criterion

The CESAR-LCPC software does not provide the values of the safety coefficients necessary to assess the surface stability after certain breaking criteria. Therefore, we will introduce such a criterion, starting from the intrinsic curve of the rock. For a certain point, characterized by a certain state of tension, the corresponding Mohr circle is determined and is reported to the intrinsic curve of the rock salt. In this sense, we will consider Mohr-Coulomb's right (defined by the relationship: $\tau = C - \sigma \cdot tg\phi$) and the following conditions will be determined:

a) If $\sigma_1 < R_t$, for $R_1 = \left(C \cdot ctg\phi - S_c\right) \cdot \sin\phi$ result $CS = R_1 / R$;

b) If $\sigma_1 \geq R_t$, then $CS = 0$

where: $S_c = \frac{\sigma_1 + \sigma_2}{2}$ represents the abscissa of the Mohr's circle; $R = \frac{\sigma_1 - \sigma_2}{2}$ is the radius of Mohr's circle; R_1 – the radius of Mohr's tangent circle to the Mohr-Coulomb's right; *CS* – safety coefficient; R_t – tensile strength of the rock salt; *C* – cohesion of rocks; ϕ – the internal friction angle of the rock salt.

Regarding the calculated value of the safety coefficient CS, there are three cases of stability, namely:

1) CS = 1, when the Mohr circle and the intrinsic curve are tangent – resulting in stability at the limit;
2) CS < 1, when the Mohr circle and the intrinsic curve are secant – resulting conditions for the occurrence of breaking phenomena;
3) CS > 1, when the stress state is far from the breaking phenomena – resulting in a certain degree of stability, depending on the value of the safety coefficient.

In our case, to assess the stability of the cavern after its internal contour and implicitly for the calculation of the safety coefficient CS (when: *C* = 4000 kN/m^2 and $\phi = 30^o$), we will have the relation:

$$R_1 = 3464{,}102 - 0{,}5 \cdot S_c \qquad (2)$$

The values of the safety coefficients obtained for the two sections taken into the study (section 3-3 and section 6-6) in the four considered variants of calculation are graphically shown in figures 14 - 17 in predefined sections after the surface and after the ceiling of the cavern.

Analysing the charts of the safety coefficients (see figures 14 to 17) it can be noticed that in the case of section 3-3` the safety coefficient is CS > 1, but in section 6-6` one can notice stability at the limit, the safety coefficient being CS < 1 in certain areas.

Overlapping the safety coefficient graph for Variant II of the calculation over the section 6-6`, it can be seen that in the area where the breakdown occurred in 2001, the safety factor has minimum values (Figures 18 and 19).

So, studying the last two figures, we can say that the collapse of the surface has occurred due to complex shear-traction phenomena.

Analysing the results obtained on the basis of 2D numerical modelling, it can be concluded that to the cavern dimensions recorded in 1993 the surface collapse was only a matter of time (even in some areas the safety coefficient ranges between 2 and 30, the collapse occurred in the zone where the safety coefficient it is minimal, CS < 1).

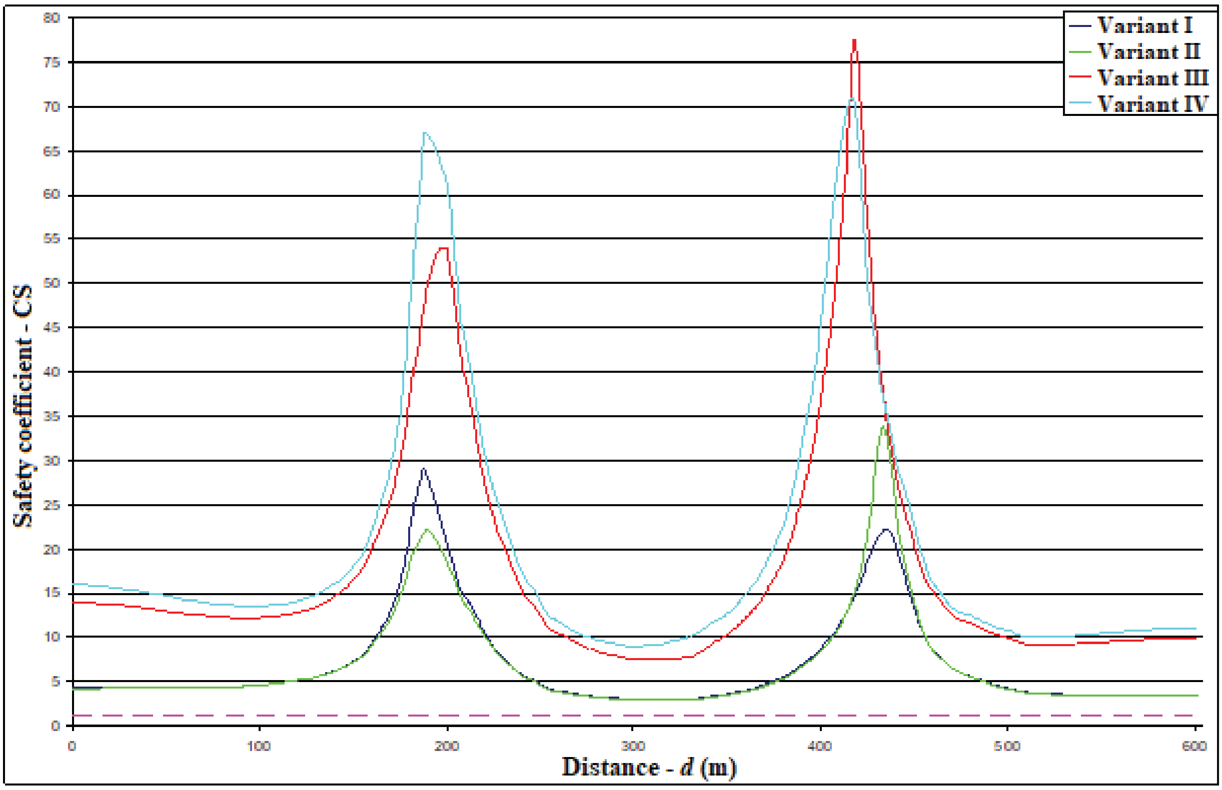

Fig. 14 *The safety coefficient along the surface in section 3-3`*

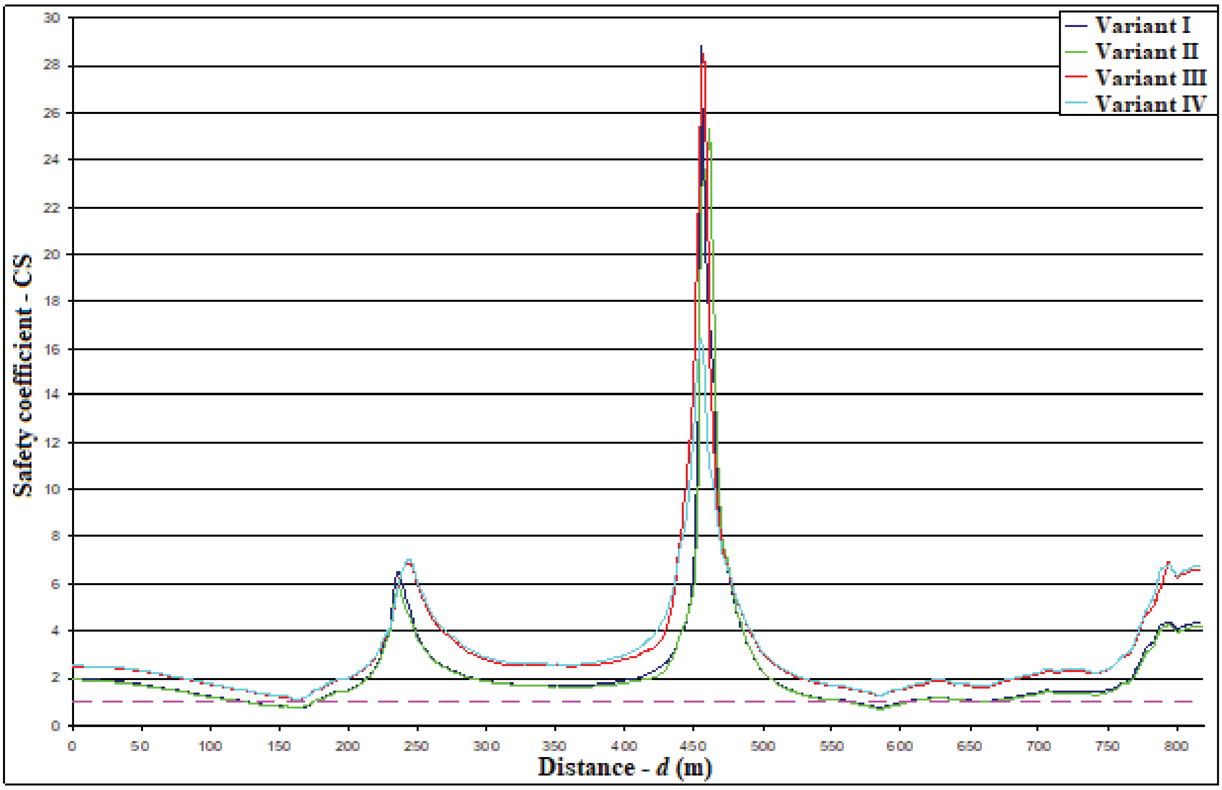

Fig. 15 *The safety coefficient along the surface in section 6-6`*

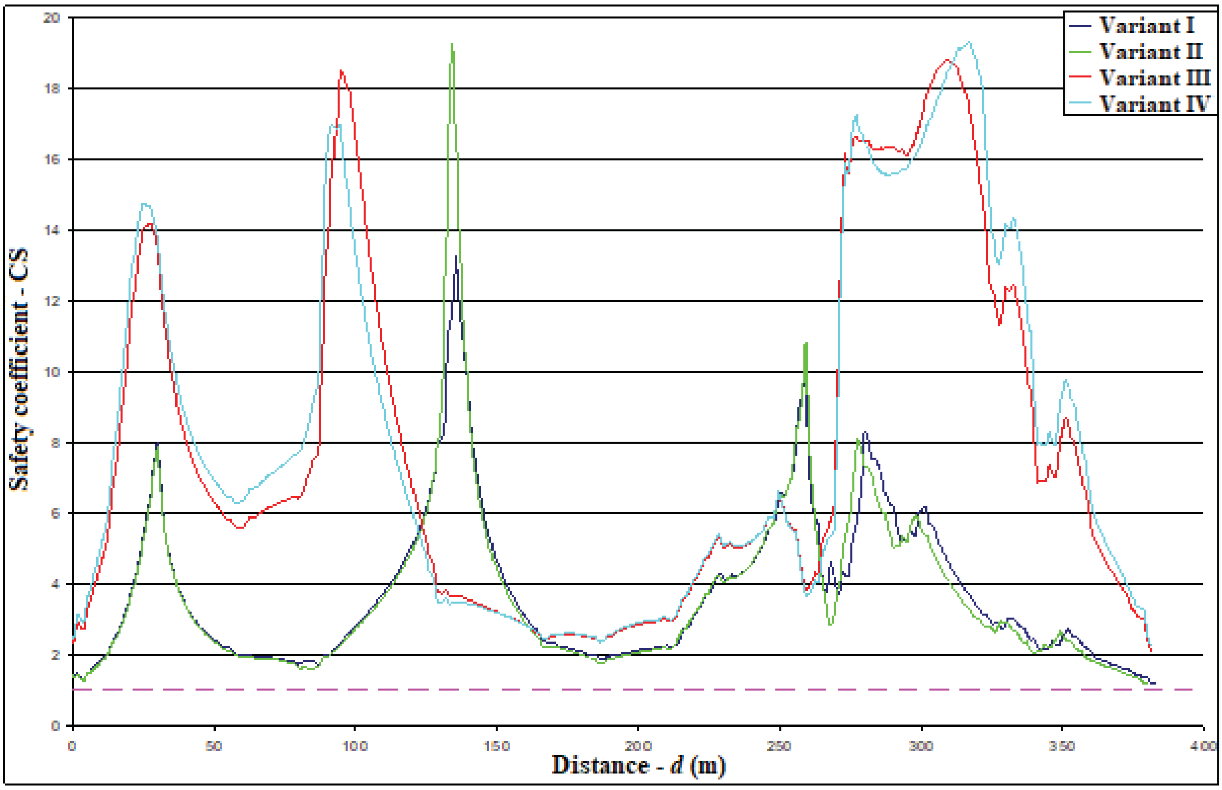

Fig. 16 *The safety coefficient along the cavern's ceiling in section 3-3`*

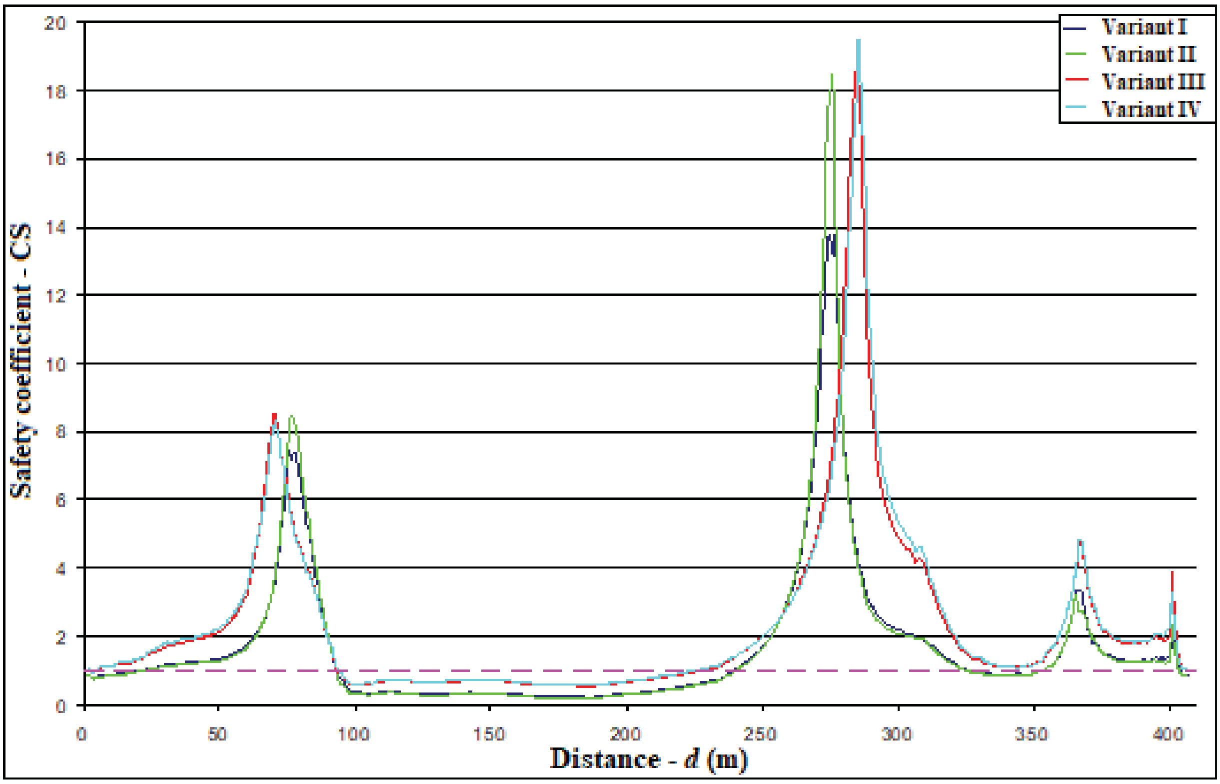

Fig. 17 *The safety coefficient along the cavern's ceiling in section 6-6`*

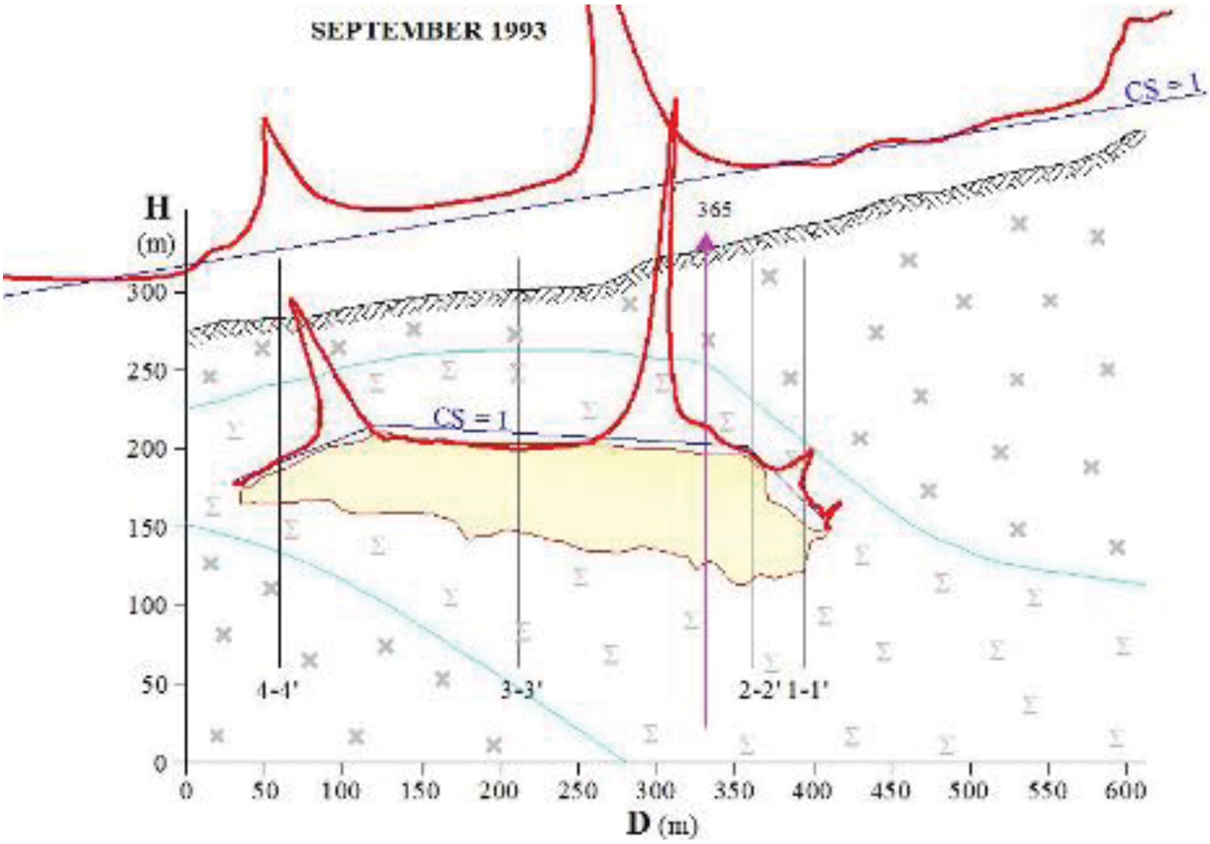

Fig. 18 *The safety coefficient along the surface and at the ceiling of the cavern in section 6-6` (September 1993)*

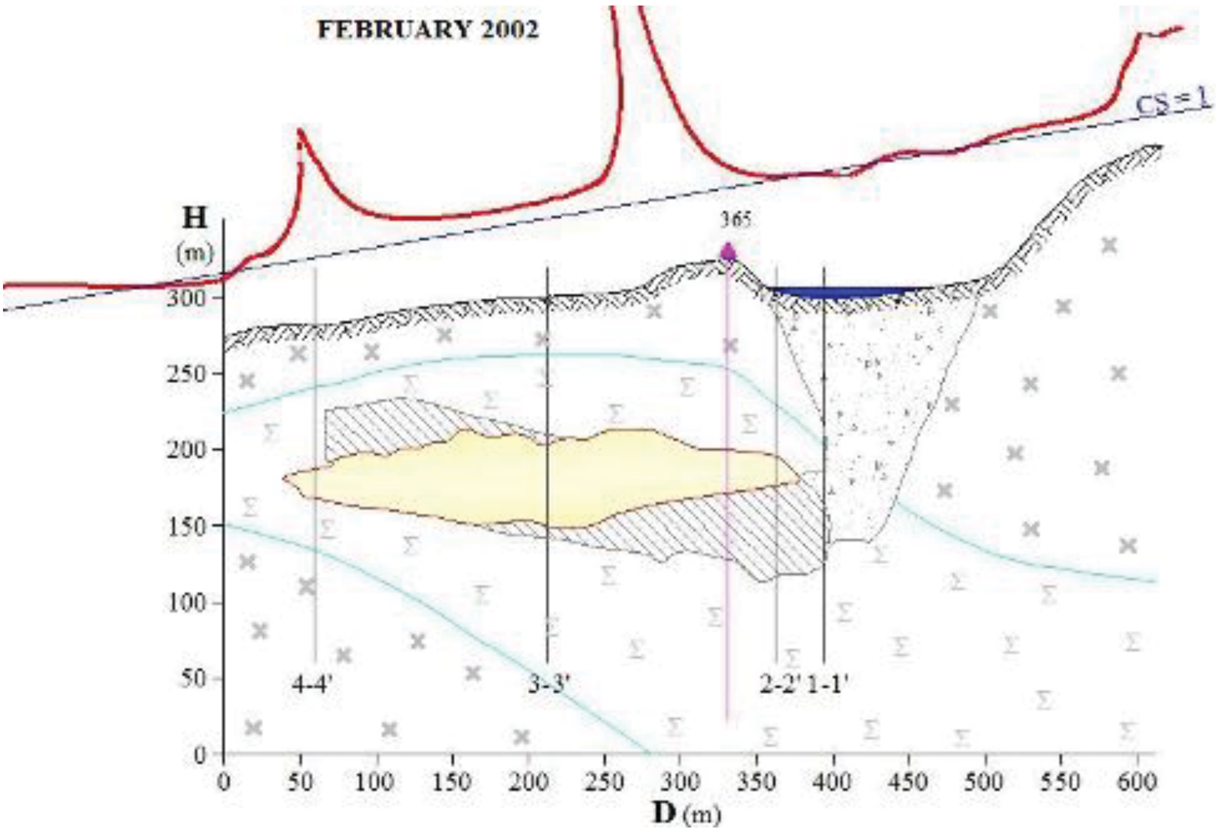

Fig. 19 *The safety coefficient along the surface in section 6-6` (February 2002)*

4. Conclusions

The analysis of the SOCON cavern stability (Ocnele Mari, Romania), by 2D numerical modelling with finite elements, was done with the help of the CESAR-LCPC software, program based on the finite element method. The 3D modelling has been avoided due to the large dimensions of the cavern (and implicitly of the model) and to the very large computing resources needed to run such a model. Also, the dimensions of the area of interest around the cavern have been determined so as to encompass the surface of the model where the variation of stresses and deformations is maximal.

The calculations were made in the elastic-plastic behaviour hypothesis of the Mohr-Coulomb type without hardening, in the case of plane deformation. For this analysis two numerical models corresponding to the vertical sections 3-3` and 6-6` were made, taking into account four possible situations, namely:

- Option I – the cavern is completely filled with brine;
- Option II – at the top of the cavern (it is considered at a height of 10 m) there is an area with air;
- Option III – the cavern is completely filled with brine and the piezometric load in the cavern is located at an elevation of + 290 m;
- Option IV – the cavern is completely filled with brine and the piezometric load in the cavern is located at an elevation of + 295 m.

From the results of this analysis, it was found that the worst situation is that in which at the ceiling of the cavern there is a gap of a certain size, but in all studied cases the tensile and shear stresses exceed the breaking strength of the rock salt.

In conclusion, it can be said that, regardless of the situation of the SOCON cavern, the collapse of the rocks from the ceiling of the cavern was inevitable, so it was necessary to implement urgent measures to avoid a disaster.

References

1. Atudorei C., Bocanete E., ş.a.
Cercetarea, exploatarea şi valorificarea sării, Editura tehnică, 1971;

2. Averşin S.G.
Cauzele deplasării terenului datorită exploatărilor miniere, Ugletehizdat, Moscova (în rusă), 1947;

3. Bendea H.
The tracing of deformations, caused by underground cavities at Ocnele Mari mining area, by topographic and calliper diameter methods, PhD Thesis, University of Petroşani.

4. Cartuta G., Portik F.
Dimensionarea planşeelor şi pilierilor de sare la exploatarea prin sonde, Buletin de topografie minieră nr. 1/1970;

5. Dima V., ş.a.
Studiu comparativ privind metoda actuală de exploatare a sării prin sonde şi metodele de exploatare în trepte şi în baterie, ICEMIN Bucureşti, 1964;

6. Gongea D., Paraschiv V., Baroncea Al.
Caracterizarea fizico-mecanică a zăcământului de sare gemă de la Ocnele Mari, C216, ICEMIN Bucureşti, 1971;

7. Hirian C.
Mecanica rocilor, Editura Didactică şi Pedagogică, Bucureşti, 1981;

8. Hirian C., Georgescu M., Deak Gy., Deak Şt.
Extraction of rock salt from Romania in the 21st century on ecomining principles, Estfalia Publishing House, Bucharest, (in romanian).

9. Kulle P.A.
Exploatarea zăcămintelor de sare prin dizolvare în subteran, 1957;

10. Marian D.P., Onica I., Cozma E., Mihuţ S.
Socon Cavern's Stability Analysis by using Finite Element Numerical Modelling, Annals of the University of Petroşani – Mining Engineering –, Vol. 15 (2014), ISSN: 1454-9174;

11. Mihuţ S., Marian D.P., Onica I., Cozma E.
Reducing Environmental Impact Generated by the Extraction of Rock Salt in Solution at the Ocnele Mari, Romania, Proceeding of the 15th International Multidisciplinary Scientific Geo-Conference & EXPO - SGEM 2015, Sofia, Bulgaria, June 16-25 2015, ISSN: 1314-2704; DOI:10.5593/SGEM2015/B13/S3.071.

12. Mihuţ S., Marian D.P., Onica I., Cozma E.
Stability analysis of the underground structures from the Ocnele Mari Saline, Proceeding of the 15th International Multidisciplinary Scientific Geo-Conference & EXPO - SGEM 2015, Sofia, Bulgaria, June 16-25 2015, ISSN: 1314-2704; DOI: 10.5593/SGEM2015/B13/S3.078

13. Mocuţa M.
Contribuţii la înţelegerea cauzelor şi evoluţiei proceselor de dezechilibru din Câmpul II de sonde de la Ocnele Mari. Soluţii de dezamorsare, Teză de doctorat, Universitatea din Bucureşti, Facultatea de geodezie şi Geofizică, 2005;

14. Onica, I., Marian, D.P. *Ground surface subsidence effect of underground mining as thick coal seams of the Jiu Valley in the Basin*, the Archives of Mining Sciences, Vol. 57, no. 3, p. 547-577; ISSN: 0860-7001.

15. Onica I., Marian D.P.
Applications of the finite element method in the analysis of land and underground structures stability, Universitas Publishing House, Petroșani, ISBN 978-973-741-473-1, 215p (in romanian).

16. Panet, M.
Stabilité et soutènement des tunnels, Chapitre IX de La mécanique de roches appliquée aux ouvrages de génie civil, Publication de l'Association amicale des Ingenieurs anciens élèves de l'ENPC, Aix-en-Provence.

17. Pavel M.
Documentație tehnică privind realizarea amorsării câmpului IV de sonde Ocnele Mari prin fisurare hidraulică, E.M. Râmnicu Vâlcea, 1993;

18. Popescu Al., Todorescu A.
Mecanica rocilor în minerit, Editura Tehnică, București, 1982;

19. Stamatiu M.
Mecanica rocilor, Editura Didactică și Pedagogică, București, 1962;

20. Todorescu A.
Proprietățile rocilor, Editura Tehnică, București, 1984;

21. Zamfirescu F., Danchiv A., Dima R., Popa I., Constantinescu T., Mocuța M., Niță C., Andrei M., Popescu C.
Evaluarea factorilor de risc din zona câmpurilor de sonde I – IV Ocnele Mari, Contract de cercetare, Universitatea București, 2005;

22. Zamfirescu F., Danchiv A., Constantinescu T., Mocuța M., Andrei M., Niță C.
Monitorizarea Câmpurilor I-IV de sonde Ocnele Mari – Raport anual, Contract de cercetare, Universitatea București, 2011;

23. ***
Manualul inginerului de mine, Vol. I, Editura tehnică, București, 1984;

24. ***
Mining Engineering Handbook, New York, 1973;

Scientific reviewer
Lect.eng.Ph.D. Ladislau RADERMACHER
UNIVERSITY OF PETROȘANI